

DNA translocation through α -hemolysin nanopores with potential application to macromolecular data storage

Cite as: J. Appl. Phys. **97**, 104317 (2005); <https://doi.org/10.1063/1.1905791>

Submitted: 20 December 2004 . Accepted: 17 March 2005 . Published Online: 06 May 2005

Pramod K. Khulbe, Masud Mansuripur, and Raphael Gruener



View Online



Export Citation

ARTICLES YOU MAY BE INTERESTED IN

[Polymer capture by electro-osmotic flow of oppositely charged nanopores](#)

The Journal of Chemical Physics **126**, 164903 (2007); <https://doi.org/10.1063/1.2723088>

[Ion selection of charge-modified large nanopores in a graphene sheet](#)

The Journal of Chemical Physics **139**, 114702 (2013); <https://doi.org/10.1063/1.4821161>

[Electrical characterization of protein molecules by a solid-state nanopore](#)

Applied Physics Letters **91**, 053901 (2007); <https://doi.org/10.1063/1.2767206>

Applied Physics Reviews
Now accepting original research

2017 Journal
Impact Factor:
12.894

DNA translocation through α -hemolysin nanopores with potential application to macromolecular data storage

Pramod K. Khulbe^{a)} and Masud Mansuripur
Optical Sciences Center, University of Arizona, Tucson, Arizona 85721

Raphael Gruener
Department of Physiology, University of Arizona, Tucson, Arizona 85721

(Received 20 December 2004; accepted 17 March 2005; published online 6 May 2005)

Digital information can be encoded in the building-block sequence of macromolecules, such as RNA and single-stranded DNA. Methods of “writing” and “reading” macromolecular strands are currently available, but they are slow and expensive. In an ideal molecular data storage system, routine operations such as write, read, erase, store, and transfer must be done reliably and at high speed within an integrated chip. As a first step toward demonstrating the feasibility of this concept, we report preliminary results of DNA readout experiments conducted in miniaturized chambers that are scalable to even smaller dimensions. We show that translocation of a single-stranded DNA molecule (consisting of 50 adenosine bases followed by 100 cytosine bases) through an ion channel yields a characteristic signal that is attributable to the two-segment structure of the molecule. We also examine the dependence of the translocation rate and speed on the adjustable parameters of the experiment. © 2005 American Institute of Physics. [DOI: 10.1063/1.1905791]

I. INTRODUCTION

Digital information can be encoded in the building-block sequence of macromolecules, such as RNA and single-stranded DNA. In principle, the four nucleotides of DNA, for example, can be used to represent a 2-bit sequence (e.g., $A=00$, $C=01$, $G=10$, and $T=11$), although practical considerations may impose certain restrictions on the specific sequences that can be used to encode the information. A data storage device built around this concept must have the ability to (i) create macromolecules with any desired sequence of building blocks, i.e., write or encode the digital information into macromolecular strands; (ii) analyze and decode the sequence of a previously created macromolecule, i.e., read the recorded information; and (iii) provide an automated and reliable mechanism for transferring the macromolecules among the read station, the write station, and designated locations (parking spots) for storing each such macromolecule. Although methods of writing and reading macromolecular strands are currently available (e.g., arbitrary sequences of oligonucleotides can be synthesized, and DNA sequences can be deciphered), these methods require large machines and are slow and expensive. In an ideal molecular data storage system, routine operations such as write, read, erase, store, and transfer must be carried out within an integrated chip, reliably and at high speed.

As a possible alternative to present-day mass data storage devices (e.g., magnetic and optical disks and tapes), we envision a system in which data blocks are encoded into macromolecules constructed from two or more distinct bases, say, x and y ; the bases can be strung together in arbitrary

sequence such as $xyxyxyxy \cdots xyx$ to represent binary sequences of user data (e.g., $x=0$, $y=1$).^{1,2} The macromolecular data blocks must be created in a *write station*, transferred to *parking spots* for temporary storage, and brought to a *read station* for decoding and readout. The “erase” operation is as simple as discarding a data block and allocating its parking spot to another macromolecule. The parking spots and read/write stations depicted in Fig. 1, for example, are microfluidic chambers connected via microchannels and microvalves (not shown) that enable automatic access through an electronic addressing scheme.² With the dimensions of the various chambers indicated in Fig. 1, one can readily incorporate, on a 1.0-cm² surface area, a total of 10^6 parking spots (~ 0.25 cm²), 1000 read/write stations (~ 0.1 cm²), and the necessary plumbing (e.g., 1- μ m-wide connecting routes and 1×1 - μ m² binary valves or switches), which would occupy an area of ~ 0.65 cm². Assuming megabyte-long data blocks, the storage capacity of the 10^6 parking spots in this scheme will be 10^{12} bytes/cm². In a three-dimensional design based on 10- μ m-thick layers, the capacity of the proposed molecu-

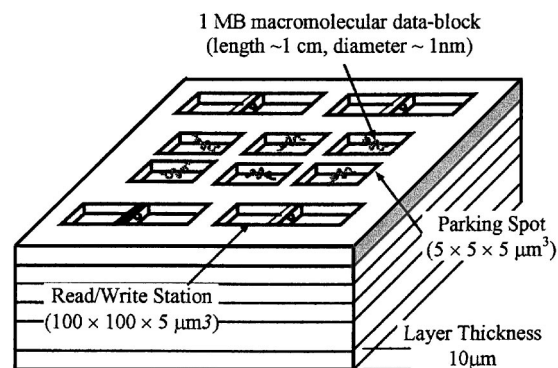


FIG. 1. Chip surface area utilization. The same arrangement of read/write stations and parking spots is repeated in stacked layers.

^{a)}Author to whom correspondence should be addressed; electronic mail: pkkhulbe@u.arizona.edu

lar storage system would exceed 10^{15} bytes/cm³.

Presently, secondary storage of data is the domain of magnetic hard disks, removable magnetic media (e.g., zip disk and magnetic tape), optical disk drives [e.g., compact disk-recordable (CD-R) and digital versatile disk-rewriteable (DVD-RW)], and magneto-optical media. All these storage technologies are inherently two dimensional in the sense that information is recorded on a thin layer at the surface of a disk or a tape medium. Considering possible advances in read/write heads and media technology, current methods of data storage can be (optimistically) pushed to densities in the range of 75–150 GB/cm². Going beyond this range, however, will be problematic owing to the fundamental physical limitations. The optical storage technology is exemplified by DVD-RW, a 12-cm-diameter platter having a capacity of 4.7 GB. The next-generation DVDs are expected to use blue lasers (wavelength ~ 400 nm) and have a capacity of ~ 25 GB per platter. Double layer disks with capacities of ~ 50 GB are also feasible. Beyond this, the optical drives planned for the year 2010 and beyond are expected to have capacities in excess of 100 GB, although several technical hurdles must be overcome before such devices can even be demonstrated in the laboratory. To summarize, both magnetic and optical recording technologies have the potential for terabyte capacity, but it is highly doubtful that these technologies can reach into the petabyte domain. The concept proposed in this paper has the potential to revolutionize information storage at extremely high density and rapid retrieval rates required for massive databases of the future. For a comparison with a current state-of-the-art technology, note that storing 10^{15} bytes of data on conventional DVDs requires a 128-m-tall stack of these 12-cm-diameter platters; the same amount of data that the 1-cm³ molecular data storage device of Fig. 1 is expected to be able to handle.

In an effort to demonstrate the feasibility of the proposed molecular storage scheme, we have built miniaturized read stations for DNA strands.^{2,3} The idea is to translocate single-stranded DNA molecules through a nanopore while monitoring the variations of the electrolytic current through the pore, as has been described elsewhere in the context of gene analysis and sequencing.^{4–11} Whereas in decoding a genome the DNA sequence could be arbitrary, in the proposed data storage application it is possible to tailor the sequence to the characteristics of the read station. For instance, if the electrical signals corresponding to individual bases turn out to be indistinguishable [due to insufficient signal-to-noise ratio (SNR) or because the ion channel is too long compared to the dimensions of single nucleotides], one might instead associate the information bits with strings of identical bases; for example, a string of 20 adenosines can be used to represent a 0, while a string of 30 cytosines could represent a 1.

II. MATERIALS AND METHODS

Our read stations, complete with electrodes and access ports, were molded from polydimethylsiloxane (PDMS), cast in a machined Teflon block. This design, which is scalable to even smaller dimensions, allows easy integration with mul-

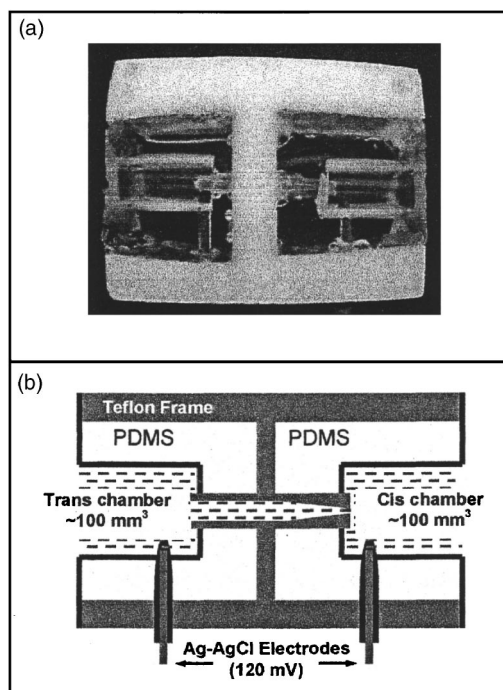


FIG. 2. (a) Photograph and (b) diagram of a read station built inside a 10-mm-thick H-shaped Teflon frame. A Teflon tube, shrunk at one end to a 20- μ m-diameter aperture, goes through the central wall and forms a tight seal between the *cis* and *trans* chambers. The 6-mm-long, 4.6-mm-diameter cylindrical chambers are large enough to hold the buffer solution for several hours; evaporation reduces the buffer by 50% in 24 h. The chambers are connected to an Axopatch 200B amplifier via Ag–AgCl electrodes. The 20- μ m-diameter aperture holds a (vertical) lipid bilayer, into which one or more α -HL ion channels are implanted. Single-stranded DNA molecules are driven through the channel by an applied voltage in the range of 90–210 mV, positive at the *trans* side.

multiple parking spots on the same chip. In the read station depicted in Fig. 2, the needlelike end of the tube that connects the *cis* and *trans* chambers was covered with a Teflon cap (aperture diameter ~ 20 μ m) to promote the formation of a lipid membrane over the aperture. The nanopore, self-assembled in the lipid membrane from seven subunits of α -hemolysin (α -HL) protein, is a 10-nm-long ion channel, whose cap (length ~ 5 nm) resides in the *cis* chamber, while its 5-nm-long stem spans the lipid membrane. The ion channel has an opening diameter of 2.6 nm at the entrance to the cap, 1.5 nm in the constricted region in the middle, and 2.2 nm at the far end of the stem located in the *trans* chamber.^{4,5}

In the read station of Fig. 2, the *cis* chamber is accessed (under microscope control) with a micropipette from the right-hand side, and the *trans* chamber from the left-hand side. The micropipette is used for filling the chambers with buffer, adding α -HL or DNA to the *cis* chamber, and removing the additives by perfusion. At 50- μ L volume (partial filling), the chambers are small enough to yield a low-noise electrolytic current signal, yet large enough to avoid problems associated with the evaporation of the liquids. If the device dimensions were to shrink further, both chambers would have to be capped to prevent evaporation.

The buffer used in our experiments was 1-M KCl, 10-mM 4-(2-Hydroxyethyl)piperazine-1-ethanesulfonic acid

(HEPES) (pH \sim 8.0), pH balanced by KOH, and the lipid was diphytanoyl phosphatidycholine (DPC). The Ag–AgCl electrodes were made by dipping a silver wire in Clorox. The patch-clamp amplifier was Axon Instrument's Axopatch 200B.

Prior to filling the chambers with buffer, 2 μ L of a lipid solution in hexane (1.5 mg/mL) is released in the vicinity of the 20- μ m aperture between the *cis* and *trans* chambers. The chambers are then dried under a mild stream of nitrogen, thus allowing a thin layer of lipid to coat the surrounding walls without clogging the aperture. Care must be taken to completely evaporate the hexane, as even trace amounts in the aperture area can ultimately destroy the bilayer. We found that the lipid bilayer that must cover the aperture between the two chambers does not form properly when applied to a PDMS surface. Although PDMS is hydrophobic—a requirement for this application—its porosity ultimately destroys the lipid membrane a few minutes after the formation of a bilayer. In the read station depicted in Fig. 2, the needlelike end of the tube that connects the *cis* and *trans* chambers had to be covered with a Teflon cap (aperture diameter \sim 20 μ m) to form a stable lipid membrane.

The *cis* and *trans* chambers (as well as the tube that connects them) are subsequently filled with buffer. We soaked 1.5 mg of lipid in 5 μ L of hexadecane in a test tube for 60–90 s; the leftover hexadecane was then completely drained, leaving a viscous lipid at the bottom of the tube. A microcapillary tube (inner diameter \sim 300 μ m) was filled to 1-mm height from its tip with this viscous lipid in such a way as to form a convex meniscus at the tip of the capillary. Using a micromanipulator, this lipid meniscus was brushed across the 20- μ m aperture with a slight pressure. A 60 Hz, 5-mV square wave was then applied between the Ag–AgCl electrodes across the bilayer (the so-called seal test) to verify that the bilayer is adequate. The above procedure succeeds in creating a proper bilayer across the aperture in about 90% of the trials.

Once a stable bilayer was obtained, 40 ng of α -HL protein was dissolved in 2 μ L of buffer and added to the *cis* chamber. Applying a 120-mV potential across the bilayer enables one to observe the reconstitution of an ion channel into the bilayer, an event which is indicated by an abrupt jump of the current from 0 to \sim 120 pA. The observed voltage-to-current ratio of \sim 1.0 G Ω is consistent with the single-channel conductance of α -HL nanopores under similar conditions, as reported in the literature.⁵ Self-assembly of a single-ion channel within the lipid membrane typically takes 20–30 min, after which the excess α -HL is removed by perfusion with 10 mL of fresh buffer.

Two different oligodeoxynucleotide samples were used in our experiments: the 5'*A*₅₀*C*₁₀₀3', with a total of 150 base units/molecule, was used in the experiment described in Fig. 4. All other experiments (reported in Figs. 5–10) used 5'(AC)₆₀3', with a total of 120 bases/molecule. Both custom-synthesized, polyacrylic gel electrophoresis (PAGE) grade samples were purchased from Midland Certified Reagent Company (Midland, Texas). The samples were sus-

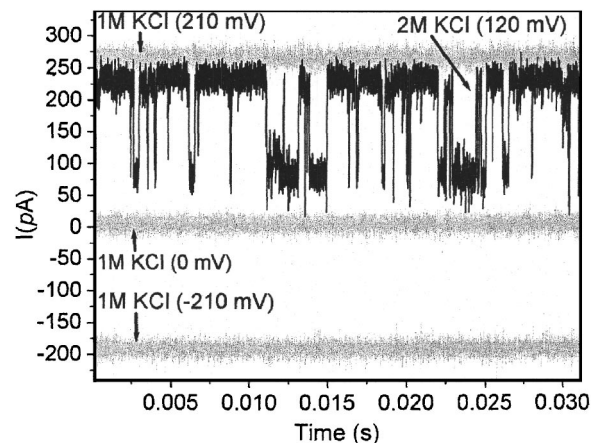


FIG. 3. Current traces obtained from a reconstituted α -HL channel incorporated into a bilayer. The gray traces show the channel in the nonconducting state (0 mV), forward conducting state (210 mV), and reverse-biased state (-210 mV), in the presence of 1-M KCl on both sides of the bilayer. Note the difference in the current level between the $+210$ - and -210 -mV traces, which indicates the channel's asymmetric response to a polarity reversal of the applied voltage. In the presence of 2-M KCl, and in response to an applied voltage of $+120$ mV (black trace), the channel fluctuates spontaneously between the open and closed states—a behavior known as channel gating.

ended in TE buffer [10-mM tris/1-mM ethylenediamine tetraacetic acid (EDTA)] at pH 8.0, before being released into the *cis* chamber, where the final concentration of 5'*A*₅₀*C*₁₀₀3' was 7.15 nM/ml, while that of 5'(AC)₆₀3' was 14.3 nM/ml.

III. RESULTS

A. Gating behavior of α -hemolysin nanopore at high KCl concentration

One of our goals was to improve the SNR of readout by increasing both the KCl concentration in the buffer and the applied voltage. The increased salt concentration, however, resulted in ion-channel gating, which is an unacceptable behavior for the observation of DNA translocation events. The higher voltage, on the other hand, helped raise the SNR by enhancing the signal without causing much increase in the noise.

The gray traces in Fig. 3 show the electrical current through a single nanopore with 1-M KCl concentration at applied voltage levels of $+210$, -210 , and 0.0 mV, respectively. The channel is always open at this KCl concentration, and the forward current is just over 250 pA, while the reverse current is about -200 pA. The width of the trace in each case is a good measure of the noise level present during the measurement. (The KCl concentration was 1 M on both *cis* and *trans* sides; in other words, there was no transmembrane gradient.)

When the KCl concentration is raised to 2 M, the ion channel exhibits a “gating” behavior, namely, it opens and closes randomly, as can be seen in the black trace in Fig. 3. The applied voltage was reduced in this case to $+120$ mV to make the forward current (in the open state of the ion channel) nearly equal to the forward current in the case of 1-M KCl concentration. (At 2-M KCl, a gating behavior was also observed at higher voltages, up to 200 mV, and also when a

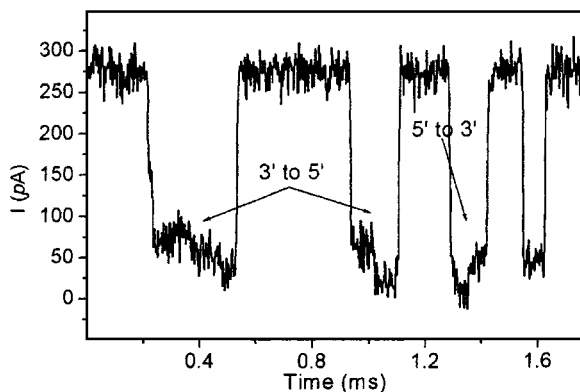


FIG. 4. Effects of ssDNA passage through the α -HL channel on current flow. Single-stranded DNA having a sequence of $5'A_{50}C_{100}3'$ was introduced into the *cis* chamber (where the cap of the reconstituted ion channel is located). The buffer concentration was 1-M KCl, the applied voltage was +210 mV, and the amplifier bandwidth was 100 kHz. The channel's open state is seen to be interrupted by four brief closures (i.e., translocation events). The first and second events show two closure substates indicating the translocation of ssDNA from the 3' end to the 5' end. The third event also shows two substates which, however, are reversed, indicating the passage of the ssDNA from the 5' end to the 3' end. The A_{50} and C_{100} sections of the molecule are not distinguishable in the fourth event.

reverse voltage, $V=-120$ mV, was applied.) Apparently, at some KCl concentration between 1 and 2 M, the nanopore exhibits gating, irrespective of the level or polarity of the applied voltage.

B. Translocation of $5'A_{50}C_{100}3'$ single-stranded DNA

The single-stranded DNA (ssDNA) molecules traversed the ion channel under $V=210$ mV at 1-M KCl buffer concentration, and were observed with the amplifier bandwidth set to 100 kHz. In one trial, of the 171 translocation events monitored, 49 events, or nearly 29%, showed a bilevel behavior. (Not every event is expected to exhibit a bilevel signal, either due to the large fluctuations of the blockade current or because of incomplete translocation, in which the molecule is trapped in the vestibular region of the α -HL cap for a certain length of time, then returned to the *cis* chamber without traversing the ion channel.) The bilevel behavior is seen in three of the four events shown in Fig. 4. Translocation duration for the entire molecule is typically ~ 150 μ s. In some instances, such as the first event in Fig. 4, the molecule appears to get stuck in the midst of translocation, which results in a longer-than-average transition time. The fourth event in Fig. 4 is typical of the remaining 71% of events in which either the molecule entered the pore but did not complete translocation or the bilevel signal was not clearly visible due to insufficient SNR. (It is worth mentioning that, in our experiments, the bilevel signals were *not* observed for $V=120$, 150, or 180 mV; the higher level of the applied voltage, $V=210$ mV, was necessary to obtain these signals.) Although bilevel translocation signals from two-segment RNA molecules have been reported in the literature,⁸ we are not aware of any such results in the published record for ssDNA.

It has been shown by several research groups that, for a given polynucleotide, translocation events generally fall into two categories, with one group of events showing less cur-

rent blockade than the other. This grouping has been suggested to arise from the translocation of the molecule in either of the two orientations, namely, $3' \rightarrow 5'$ or $5' \rightarrow 3'$, or it might represent the translocation of the polymer in one of the two different structural conformations.⁵⁻⁹ An asymmetric interaction between the polynucleotide and the internal pore structure has been suggested as the cause of the observed grouping in those occasions where the entry of the molecule into the pore from its 5' end produces a larger current blockade than when the 3' end enters the pore first.¹²

In our $5'A_{50}C_{100}3'$ ssDNA sample, keeping in mind the fact that the *C* nucleotide is smaller than the *A* nucleotide, the 100-base-long *C* segment is expected to drop the ionic current somewhat less than the 50-base-long *A* segment does. The order in which the high and low portions of the bilevel signal occur during each translocation event depends on whether the 3' end or the 5' end of the molecule enters the nanopore first. Of the 29% bilevel events observed in the aforementioned experiment, nearly three quarters were associated with the *C* segment entering first, during which events the average normalized current, $\langle I_{\text{blocked}}/I_{\text{open}} \rangle$, was 0.37 ± 0.09 for the *C* segment and 0.17 ± 0.04 for the *A* segment. In the remaining quarter of the bilevel events (associated with the *A* segment entering first) the average normalized current was 0.20 ± 0.03 for the *C* segment and 0.12 ± 0.04 for the *A* segment. These results are consistent with the aforementioned suggestion that the entry of polynucleotides into the pore from their 5' end causes a larger current blockage than entry from the 3' end.

The preceding statements based on only 49 complete threading events are admittedly inadequate, as such measurements are inevitably subject to large statistical variations. Our intent here has been a demonstration of the "possibility" of encoding and decoding bilevel signals using single-stranded DNA molecules. A detailed understanding of the processes involved obviously requires extensive measurements and detailed statistical analysis, which will require a separate study in its own right.

C. Effect of increased voltage

Both the capture rate of the DNA molecules and the translocation speed through a single-ion channel were found to be strong functions of the applied voltage V , as has been reported by other researchers as well.^{5,13} The three frames in Fig. 5 represent the translocation of 120-base-long $5'(AC)_{60}3'$ DNA molecules under the influence of three different voltages. At $V=150$ mV, the average open-channel current is $\langle I_{\text{open}} \rangle \sim 160$ pA, and many translocation events are seen to occur. At $V=120$ mV and $\langle I_{\text{open}} \rangle \sim 130$ pA, the translocation rate has declined, and at $V=90$ mV, $\langle I_{\text{open}} \rangle \sim 90$ pA, the events are relatively rare.

The observed behavior may indicate that the increased voltage has somehow directed a large number of DNA molecules (that would otherwise drift away from the vicinity of the pore) toward the ion channel. This, in turn, is a clue concerning the transport mechanism of DNA molecules toward the pore, namely, that the drift of the molecule is not entirely controlled by thermal diffusion, and that the cham-

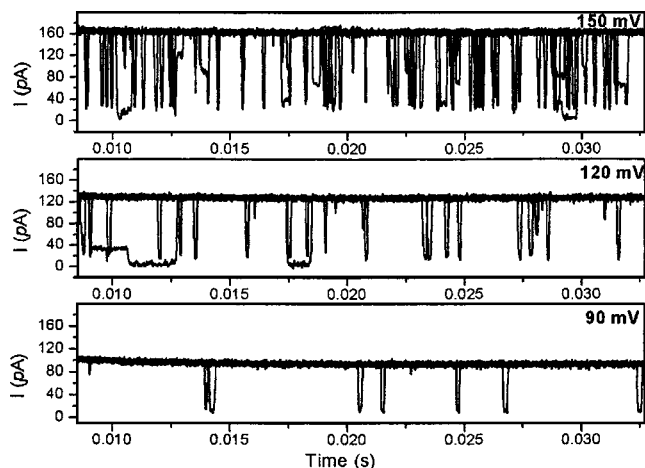


FIG. 5. Translocation of 120-base-long $5'(AC)_{60}3'$ DNA molecules under three different applied voltages. There are seven overlapping traces at each voltage corresponding to a total translocation time of 170 ms. At $V = 150$ mV, $\langle I_{\text{open}} \rangle \sim 160$ pA and translocation events are frequent. At $V = 120$ mV, $\langle I_{\text{open}} \rangle \sim 130$ pA and translocation rate has declined. At $V = 90$ mV, $\langle I_{\text{open}} \rangle \sim 90$ pA and the events are rare.

ber geometry and placement of the electrodes can influence (and perhaps even control) the motion of DNA strands toward the ion channel. When considering this particular method of molecular readout in the context of data storage, it must be remembered that, since individual macromolecules are required to travel between their parking spots and the read/write stations, controlled molecular transport is of utmost significance.

Figure 6 shows some of the statistics of the translocation experiment depicted in Fig. 5. Figure 6(top) shows that at lower applied voltages the ion channel is open (i.e., not clogged by a translocating molecule) for a larger fraction of time than at higher voltages. According to Fig. 6(bottom), the translocation rate (i.e., number of events per second), whether complete (■) or incomplete (●), is an increasing function of the applied voltage. The total translocation rate (▲), which is the sum of complete and incomplete translocations per second, increases nearly threefold between $V = 120$ mV and $V = 150$ mV.

Figure 7 shows the distribution of the event duration ΔT versus the current blockage in the experiment of Fig. 5. These data indicate that, at higher applied voltage, there is less current blockage, perhaps because the molecules are likely to be linearized, thus presenting a smaller cross section to the pore. Also, at higher applied voltage the translocation duration is reduced, meaning that the molecules travel faster through the ion channel. The speed of the molecules passing through the nanopore is seen to be roughly proportional to the applied voltage, as has been reported elsewhere.^{5,9} Faster translocation, of course, is desirable for the data storage application as it results in a greater data-transfer rate, so long as the SNR remains reasonably high at the correspondingly larger bandwidth.

D. Experiments with multiple nanopores

In a typical nanopore experiment, α -HL proteins are removed (by perfusion) from the *cis* chamber immediately af-

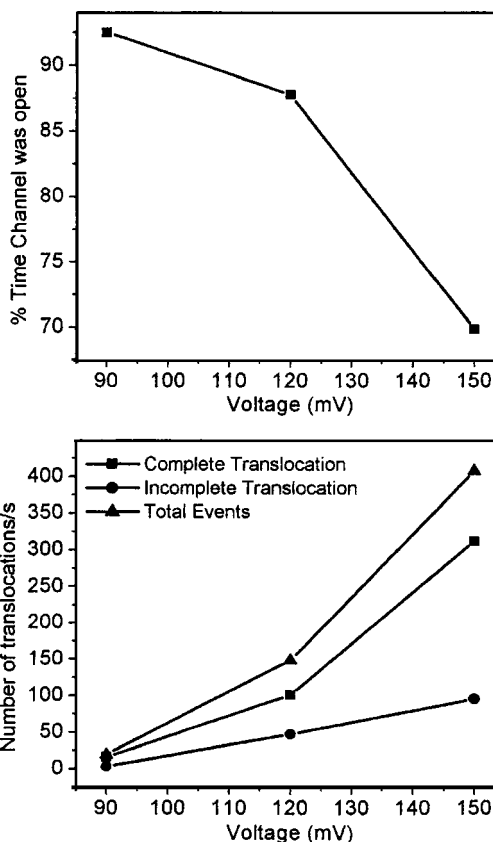


FIG. 6. Characteristics of translocation events in the experiment depicted in Fig. 5. (Top) Fraction of time during which the ion channel is open (i.e., not clogged) as function of the applied voltage V . (Bottom) Translocation rate vs applied voltage.

ter the formation of a single nanopore. Given sufficient time, however, additional ion channels reconstitute themselves in the same lipid membrane. In one experiment, the lipid bilayer had a diameter of $20 \mu\text{m}$, resulting in a pairwise sepa-

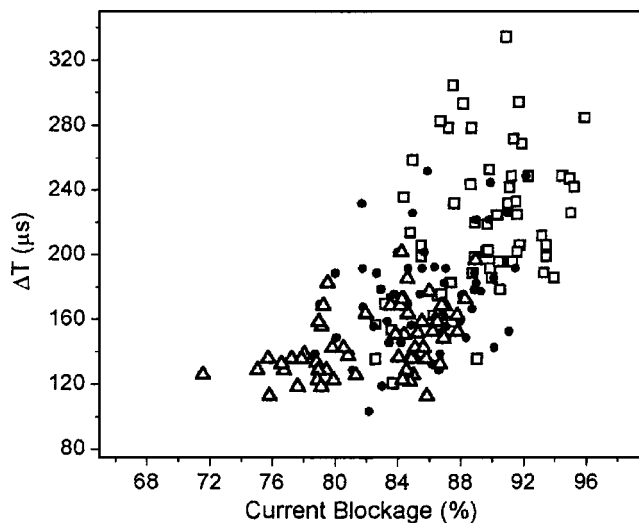


FIG. 7. Statistics of translocation events in the experiment depicted in Fig. 5. The percentage current blockage is shown on the horizontal axis, while the duration of the event appears on the vertical axis. The cluster of the open triangles represents the case of applied voltage $V = 150$ mV, the solid circles correspond to $V = 120$ mV, and the open squares represent the case of $V = 90$ mV.

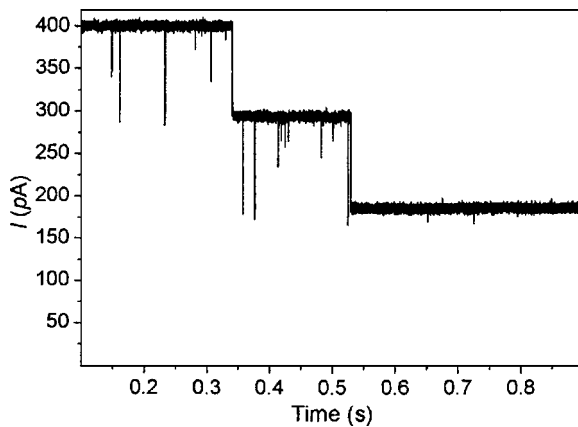


FIG. 8. A typical trace of the electrolytic current obtained when three ion channels (reconstituted in the same lipid membrane) operate simultaneously and independently of each other. When a DNA molecule is stuck in one of the nanopores, the current drops to ~ 290 pA. With two nanopores similarly clogged, the total current across the membrane is ~ 190 pA. The complete translocation events are found to have average rates of 12.6, 6.2, and 3.3 events/s, with zero, one, or two nanopores clogged, respectively. The corresponding rates for partial events in these three cases are 19.2, 13.5, and 7.0 events/s, leading to total event rates of 31.8, 19.7, and 10.3/s.

ration of at most $20 \mu\text{m}$ between nanopores. Figure 8 shows a typical trace of the electrolytic current across the membrane where, initially, the total current is ~ 400 pA, indicating the presence of three open nanopores. With all three channels open, the rate of capture and/or translocation is relatively high (31.8 events/s). When one of the pores is temporarily clogged, the current drops to ~ 290 pA, and the rate of capture/translocation through the two remaining open pores drops to ~ 19.7 /s. Similarly, when two of the nanopores are clogged, the current drops to ~ 190 pA and the event rate declines to ~ 10.3 /s. These data indicate that, for each nanopore, the electrolytic current is ~ 130 pA in the open-channel state and ~ 30 pA in the clogged state. The observed capture and/or translocation rate ratio of nearly 3:2:1 confirms that the three ion channels operate independently of one another on drifting DNA molecules. We have observed the same behavior repeatedly: the event rate increased after reversing the applied voltage to clear the clogged channel(s), only to drop again with the next clogging.

In another multiple nanopore experiment, we constituted two forward nanopores as well as one reverse nanopore in the lipid membrane, then translocated DNA strands from the *cis* to the *trans* chamber and back again to the *cis* chamber. This experiment requires the addition of α -HL proteins to the *trans* chamber (to facilitate reverse nanopore formation), followed by perfusion removal of the excess α -HL. The presence of the long, narrow Teflon tube in the system of Fig. 2, however, makes it difficult to run the above protocol, since a sufficient number of α -HL molecules cannot easily diffuse through the tube (from the *trans* chamber to the lipid membrane) and also because, during perfusion, the excess α -HL cannot be readily removed from the vicinity of the membrane.

To overcome the above problems, we built the type of chamber shown in Fig. 9. In this device a $300\text{-}\mu\text{m}$ -thick Teflon sheet was perforated with a $40\text{-}\mu\text{m}$ -diameter aperture,

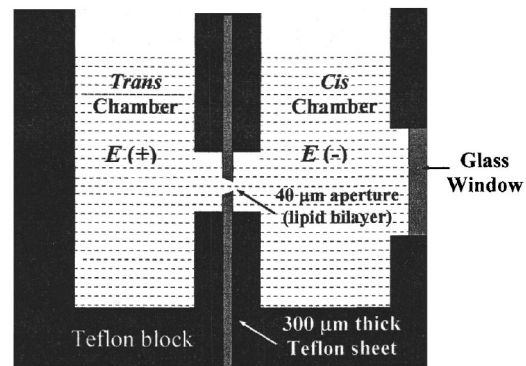


FIG. 9. Diagram of a read station designed to allow the study of back-to-back nanopores. A nanopore inserted from the *cis* side of the membrane translocates DNA molecules from the *cis* to the *trans* chamber, while a reverse nanopore (inserted from the *trans* side) returns the molecules back to the *cis* chamber on reversing the applied voltage. Two cylindrical wells (diameter= 3.8 mm, height= 7.0 mm, and volume $\sim 80 \mu\text{L}$) drilled in Teflon blocks serve as *cis* and *trans* chambers. Each block has a 2.0 -mm-diameter hole on one of its sidewalls, wherein holes are subsequently aligned face to face. The Teflon blocks are screwed together, with a $300\text{-}\mu\text{m}$ -thick Teflon sheet (perforated with a $40\text{-}\mu\text{m}$ -diameter aperture) sandwiched in between. After filling both chambers with 1-M KCl/HEPES-KOH (pH ~ 8) buffer, a lipid bilayer is formed across the $40\text{-}\mu\text{m}$ aperture; membrane formation is monitored through the glass window of the *cis* chamber. Ag-AgCl electrodes denoted by $E(+)$ and $E(-)$ are inserted from the rear side into the *cis* and *trans* chambers, then connected to an Axopatch 200B amplifier.

then sandwiched between two Teflon blocks, each having a vertical chamber (diameter= 3.8 mm and height= 7.0 mm) and a 2.0 -mm hole on the sidewall. These holes, when properly aligned, provide access to the $40\text{-}\mu\text{m}$ aperture from both the *cis* and *trans* chambers. The chambers have rear-side ports (not shown) for inserting the electrodes E . The *cis* chamber is also provided with a glass window for viewing (through a microscope) the $40\text{-}\mu\text{m}$ aperture while applying the lipid bilayer. (The procedure for applying the lipid membrane is similar to that described earlier.) Once a stable bilayer had formed, we created a reverse nanopore by adding α -HL to the *trans* chamber, then removed the excess proteins by perfusion with fresh buffer. The forward nanopores were similarly constituted by adding α -HL to the *cis* chamber, followed by perfusion.

After forming two forward and one reverse nanopores, we added $5'A_{50}C_{100}3'$ ssDNA to the *cis* chamber and monitored the electrolytic current (bandwidth= 10 kHz) while a voltage pulse sequence was applied to the electrodes ($V=+120$ mV from $t=0$ to $257 \mu\text{s}$, followed by $V=-120$ mV from $t=257$ to $850 \mu\text{s}$). Out of hundreds of traces that contain forward translocations, Fig. 10 displays five traces that have at least one reverse translocation event. At $V=+120$ mV, the open state of the channels is seen to be interrupted by several brief closures, i.e., translocation events. (Also, every once in a while, one of the two forward channels gets clogged.) This behavior is similar to what was described previously. What is intriguing is that several translocation events are observed even when the applied voltage is reversed ($V=-120$ mV). Note that the number of ssDNA molecules initially introduced into the *cis* chamber is of the order of 10^{14} . After only a few hundred *cis* to *trans* translocations, we began to detect reverse translocation events. These are likely associated with those DNA molecules that,

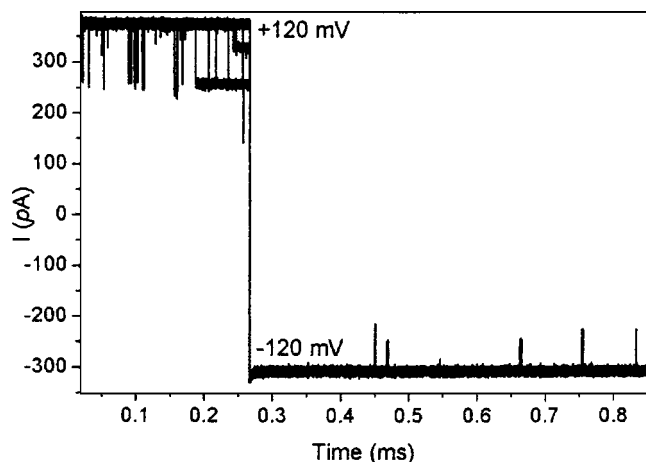


FIG. 10. Current traces obtained when two forward (*cis* to *trans*) and one backward (*trans* to *cis*) nanopores are constituted in the lipid membrane of the system of Fig. 9, then single-stranded DNA molecules are introduced into the *cis* chamber. The current was recorded when the voltage sequence $V = +120$ mV, $0 \leq t \leq 0.27$ ms; $V = -120$ mV, $0.27 \leq t \leq 0.85$ ms was applied to the electrodes. The buffer concentration was 1-M KCl, and the amplifier bandwidth was 10 kHz. When $V = +120$ mV, the open state of the channels is interrupted by several brief translocation events lasting a total of 1.35 ms (in five overlapping traces). When the voltage is switched to -120 mV, a few reverse translocations are observed (in five overlapping traces) during a 2.9-ms interval.

having been forward translocated, stay in the vicinity of the lipid membrane, then return through the reverse nanopore once the applied voltage is reversed.

The observation of reverse translocation in this experiment indicates that controlled transfer of individual molecules (e.g., from the parking lot to the read station) may be feasible, since it is the electric-field gradient, rather than random thermal drift, that is most likely responsible for the turning around (and return to the *cis* chamber) of our ssDNA molecules.

IV. CONCLUDING REMARKS

As a first step toward constructing a macromolecular data storage system, we have demonstrated the feasibility of conducting experiments with fairly short strands of DNA in a miniature read station. We showed that the *A* and *C* segments of a $5'A_{50}C_{100}3'$ ssDNA molecule can be distinguished during translocation through an α -HL ion channel. Needless to say, many hurdles must be overcome before this system can be implemented as an alternative to existing technologies.

The ultrahigh capacity is an obvious advantage of such molecular storage devices, but the data rates require substantial improvement. If the $5'A_{50}C_{100}3'$ molecules, which represent 2-bit sequences of binary information, take ~ 150 μ s to pass through a nanopore, the corresponding data-transfer rate of only 12 kbit/s would leave a lot to be desired. On the other hand, if the technology could improve to the point that individual bases could be detected during translocation, perhaps through a shorter, more robust, solid-state nanopore,^{13,14} then the achievable rate of ~ 1 Mbit/s would not be out of bounds. Moreover, if thousands of read stations could be made to operate in parallel within the same chip, the overall data-transfer rate could approach the respectable value of several Gbit/s.

Access to data is another issue that requires extensive research. Our preliminary calculations show that a 1-Mbyte-long macromolecule, enclosed in a 200-nm-diameter spherical shell (perhaps a liposome), can move electrophoretically across a 1.0-cm^2 chip in ~ 1.0 ms under a 10-V potential difference. Whether such molecules could be written and packaged on demand, within an integrated microchip, at high speed, and on a large scale, are questions to which only future research can provide satisfactory answers. Stability of the molecules over extended periods of time should obviously be a matter of concern. The lipid membrane and the proteinaceous ion channel, both being of organic origin, are ill suited for practical data storage systems; they must eventually be replaced with robust, solid-state equivalents.¹⁴

The proposed method overcomes the limitations of present-day data storage technology by creating a paradigm, thus side stepping the known obstacles to future growth in storage technology. One is no longer hampered by the superparamagnetic limit, the finite wavelength of light, the two-dimensional nature of surface recording, and other limitations of this kind. Our proposed approach also enables the creation of concepts and devices that have wide-ranging applications beyond the field of data storage. For example, rapid analysis of trace amounts of biological macromolecules, drug discovery and testing using micro-DNA synthesizer, machinery for single-chain molecular transport and manipulation, etc. Despite all the difficulties, it is our hope that this proposal will encourage debate in the pursuit of an alternative path to conventional approaches to data storage.

ACKNOWLEDGMENTS

The authors are grateful to Joseph Perry and Seth Marder of the Georgia Institute of Technology, and to Michael Hogan and Nasser Peyghambarian of the University of Arizona for many helpful discussions. This work has been supported by the Office of Naval Research MURI Grant No. N00014-03-1-0793 and by the National Science Foundation STC Program, under Agreement No. DMR-0120967.

¹M. Mansuripur, Proc. SPIE **4342**, 1 (2001).

²M. Mansuripur, P. K. Khulbe, S. M. Kuebler, J. W. Perry, M. S. Giridhar, and N. Peyghambarian, Proc. SPIE **5069**, 231 (2003).

³M. S. Giridhar, K. B. Seong, A. Schülzgen, P. K. Khulbe, N. Peyghambarian, and M. Mansuripur, Appl. Opt. **43**, 4584 (2004).

⁴D. W. Deamer and D. Branton, Acc. Chem. Res. **35**, 817 (2002).

⁵A. Meller, J. Phys.: Condens. Matter **15**, R581 (2003).

⁶M. Akeson, D. Branton, J. J. Kasianowicz, E. Brandin, and D. Deamer, Biophys. J. **77**, 3227 (1999).

⁷A. Meller, L. Nivon, E. Brandin, J. Golovchenko, and D. Branton, Proc. Natl. Acad. Sci. U.S.A. **97**, 1079 (2000).

⁸J. J. Kasianowicz, E. Brandin, D. Branton, and D. W. Deamer, Proc. Natl. Acad. Sci. U.S.A. **93**, 13770 (1996).

⁹A. Meller, L. Nivon, and D. Branton, Phys. Rev. Lett. **86**, 3435 (2001).

¹⁰S. Howorka, S. Cheley, and H. Bayley, Nat. Biotechnol. **19**, 636 (2001).

¹¹H. Bayley and P. S. Cremer, Nature (London) **413**, 226 (2001).

¹²T. A. Pologruto (private communication).

¹³P. Chen, J. Gu, E. Brandin, Y. R. Kim, Q. Wang, and D. Branton, Nano Lett. **4**, 2293 (2004).

¹⁴J. Li, M. Gershow, D. Stein, E. Brandin, and J. A. Golovchenko, Nat. Mater. **2**, 611 (2003).